



Superfluidity and Dimerization in a Multilayered System of Fermionic Polar Molecules

The Harvard community has made this
article openly available. [Please share](#) how
this access benefits you. Your story matters

Citation	Potter, Andrew, Erez Berg, Daw-Wei Wang, Bertrand Halperin, and Eugene Demler. 2010. Superfluidity and dimerization in a multilayered system of fermionic polar molecules. Physical Review Letters 105(22): 220406.
Published Version	doi:10.1103/PhysRevLett.105.220406
Citable link	http://nrs.harvard.edu/urn-3:HUL.InstRepos:7561226
Terms of Use	This article was downloaded from Harvard University's DASH repository, and is made available under the terms and conditions applicable to Open Access Policy Articles, as set forth at http://nrs.harvard.edu/urn-3:HUL.InstRepos:dash.current.terms-of-use#OAP

Superfluidity and dimerization in a multilayered system of fermionic polar molecules

Andrew C. Potter¹, Erez Berg², Daw-Wei Wang³, Bertrand I. Halperin², and Eugene Demler²

¹*Department of Physics, Massachusetts Institute of Technology, Cambridge, Massachusetts 02139*

²*Department of Physics, Harvard University, Cambridge, Massachusetts 02138 and*

³*Physics Department and NCTS, National Tsing-Hua University, Hsinchu 30013, Taiwan*

(Dated: November 30, 2010)

We consider a layered system of fermionic molecules with permanent dipole moments aligned perpendicular to the layers by an external field. The dipole interactions between fermions in adjacent layers are attractive and induce inter-layer pairing. Due to competition for pairing among adjacent layers, the mean-field ground state of the layered system is a dimerized superfluid, with pairing only between every-other layer. We construct an effective Ising-XY lattice model that describes the interplay between dimerization and superfluid phase fluctuations. In addition to the dimerized superfluid ground state, and high-temperature normal state, at intermediate temperature, we find an unusual dimerized “pseudogap” state with only short-range phase coherence. We propose light scattering experiments to detect dimerization.

PACS numbers: 05.30.-d, 03.75.Hh, 03.75.Ss, 67.85.-d

The long-range and anisotropic nature of dipole-dipole interactions offers new opportunities for ultra-cold polar molecules, beyond what is possible for cold-atom systems with only short-range, isotropic contact interactions [1]. A variety of exotic many-body states including $p_x + ip_y$ fermionic superfluids [2], and nematic non-Fermi liquids [3], are predicted to occur in cold dipolar systems. Additionally, polar molecules could provide a robust toolbox for engineering novel lattice-spin Hamiltonians [4] or hybrid devices for quantum information processing [5]. Recent progress towards trapping and cooling atoms and molecules with permanent electric or magnetic dipole moments have opened the door to exploring these exotic states of matter experimentally [6]. In order to prevent the system from collapsing due to the attractive head-to-tail part of the dipolar interaction [7], it has been proposed ([8],[9]) to create stacks of dipolar particles confined to a set of parallel planes.

In this Letter, we consider a stack of two-dimensional layers of polar fermions whose dipole moments, \vec{D} , are aligned along the stacking direction (z-axis) by an external field (see Fig. 1). The dipole-interaction, $V_d = \frac{D^2}{r^3} \left(1 - 3\frac{z^2}{r^2}\right)$, is purely repulsive between fermions in the same layer, and partially attractive (for $r < \sqrt{3}z$) between fermions in different layers. The attractive interlayer component of the dipole interaction induces BCS pairing between layers with adjacent layers competing for pairing. We demonstrate that competition between adjacent layers favors dimerization, with pairing only between even or odd pairs of layers (Fig. 1).

We find three distinct phases: a high temperature disordered phase, a fully ordered phase characterized by dimerized pairing amplitude and quasi-long range ordered (QLRO) pairing phase in each layer (Fig. 1), and a dimerized “pseudogap” phase with only short-range superfluid correlations. The latter phase is particularly interesting, since it can only be characterized by a compos-

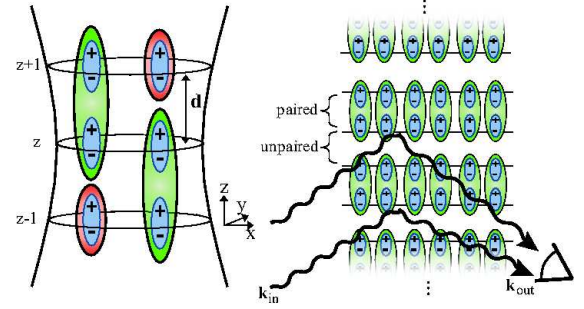


FIG. 1. Schematic representation of competition for pairing among adjacent pairs of layers, including depiction of the optical confinement beam which creates the stack of 2D sheets (left), and illustration of one of the two equivalent dimerized pairing ground states for a many layered system (right). The wavy lines illustrate the proposed light-scattering detection scheme discussed below in the text.

ite *four fermion* dimerization order parameter. Therefore, this phase does not admit a mean field (Hartree-Fock) description. This is analogous to spin nematics [10] and charge $4e$ superconductors [11], which are both phases of strongly interacting fermions that can only be characterized by composite order parameters.

Fermionic Pairing in a Layered System - The action for an N -layer system in terms of fermionic fields ψ is

$$S = \sum_{z=1}^N \sum_{\mathbf{k}} \psi_{z,\mathbf{k}}^\dagger (\partial_\tau + \varepsilon_{\mathbf{k}} - \mu) \psi_{z,\mathbf{k}} - \sum_{z,z'=1}^N \sum_{\mathbf{k},\mathbf{k}',\mathbf{q}} \psi_{z,\mathbf{k}'}^\dagger \psi_{z',\mathbf{q}-\mathbf{k}'}^\dagger V_{|\mathbf{k}-\mathbf{k}'|}^{(z,z')} \psi_{z',\mathbf{q}-\mathbf{k}} \psi_{z,\mathbf{k}} \quad (1)$$

where z and z' are (integer) layer labels, $\psi_{z,\mathbf{k}}^\dagger(\tau)$ creates a fermion with in-plane momentum \mathbf{k} and imaginary time τ in layer z . (The τ labels have been suppressed above.) $V_q^{(z,z')}$ is the dipolar interaction between layers z and z' ,

Fourier transformed with respect to the in-plane separation, for example: $V_q^{(z,z\pm 1)} = -D^2 q e^{-qd}$.

By solving the BCS gap equation: $\Delta_{z,\mathbf{k}} = -\sum_{\mathbf{k}'} V_{\mathbf{k}-\mathbf{k}'}^{(z,z+1)} \langle \psi_{z+1,-\mathbf{k}'} \psi_{z,\mathbf{k}'} \rangle$, we find that the attractive interlayer interactions induce fermionic pairing between adjacent layers z and $z \pm 1$ (see supplement for details). Interaction between next-nearest layers and beyond is small, and will be neglected throughout most of this Letter. To decouple the four-fermion interaction term, we introduce Hubbard-Stratonovich (H-S) fields $\Delta_z(\mathbf{r}_\perp)$ associated with the pairing order parameters (where \mathbf{r}_\perp is the in-plane coordinate), and integrate out the fermionic degrees of freedom [12]. Expanding the resulting fermionic determinant to quartic order (valid in the vicinity of the phase transition where $|\Delta|$ is small) yields the following Ginzburg-Landau (GL) free energy:

$$F = \sum_z \int d^2r \left(\kappa |\nabla_\perp \Delta_z|^2 + r |\Delta_z|^2 + u |\Delta_z|^4 + 2u |\Delta_z|^2 |\Delta_{z+1}|^2 \right) \quad (2)$$

where ∇_\perp denotes the gradient restricted to the xy-plane. The GL coefficients are given by $\kappa = \frac{7\zeta(3)}{32\pi^3} \frac{\varepsilon_F}{T^2}$, $r = \nu t$, and $u = \frac{1.7}{32} \frac{\nu}{T^3}$ where ζ is the Riemann zeta-function, $t = (T - T_c)/T$ is the reduced temperature, ε_F is the Fermi-energy, and ν is the two-dimensional density of states (for details we refer the reader to the supplement).

An important feature of this free energy is that the H-S expansion does not generate $|\partial_z \Delta|^2$ terms, but only terms of the form $\partial_z |\Delta|^2$. The absence of $|\partial_z \Delta|^2$ terms is not an artifact of the H-S expansion; rather, it is guaranteed by particle number conservation for each layer individually. Particle conservation for each layer stems from the absence of interlayer tunneling, and formally corresponds to N_{Layers} independent $U(1)$ phase rotation symmetries, $\psi_z \rightarrow e^{i\theta_z/2} \psi_z$, of fermion fields ψ_z in layer z . In contrast to other quasi-two-dimensional systems, such as superconducting thin films where the behavior of the system tends towards three-dimensional as the film thickness is increased, two-dimensional Berezinskii-Kosterlitz-Thouless (BKT) physics remains important even for a large number of layers.

Mean-Field Ground State - The $2u|\Delta_i|^2|\Delta_{i+1}|^2$ term in (2) indicates that adjacent pairs of layers compete with each other for pairing. For $N_{\text{layers}} > 3$, the mean-field theory predicts that it is energetically favorable for the system to spontaneously dimerize into one of two equivalent configurations where Δ vanishes between every-other layer: $|\Delta_j| = \frac{1}{2} [1 \pm (-1)^j] \Delta_0$ (see Fig.1). The situation for $N_{\text{layers}} = 3$ is more subtle, and we defer its discussion.

Effective Lattice Model for Many-Layer System - The above mean-field analysis suggests that the relevant degrees of freedom for a many-layer dipolar system are Ising-like dimerization between even or odd layers, and two-dimensional XY-like phase fluctuations of the interlayer pairing order-parameters. In order to describe

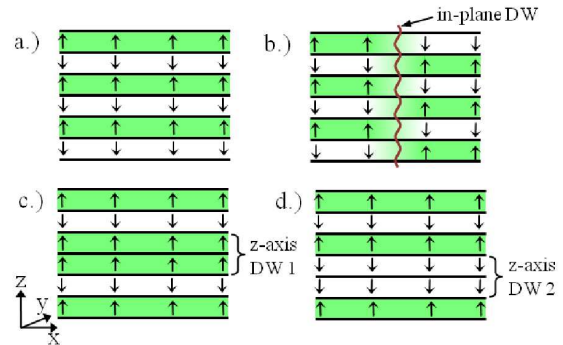


FIG. 2. Schematic depiction of fully dimerized phase (a), in-plane Ising domain-wall (DW) (b), z-axis Ising DW with pairing between two adjacent pairs of layers (c), and z-axis Ising DW with no-pairing for two adjacent pairs of layers (d). Green shading between layers indicates pairing (color online).

phase transitions in this system, we coarse-grain the GL theory (in-plane) over length-scales below the GL coherence length $\xi_{\text{GL}} \equiv (\kappa/|r|)^{1/2}$, and obtain the following effective lattice model [18]

$$F = \sum_z \left\{ K_z \sum_i \sigma_{z,i} \sigma_{z+1,i} - K_\perp \sum_{\langle ij \rangle} \sigma_{z,i} \sigma_{z,j} - \sum_{\langle ij \rangle} J(\sigma_{z,i}, \sigma_{z,j}) [\cos(\theta_{z,i} - \theta_{z,j}) - 1] \right\} \quad (3)$$

of Ising variables $\sigma_{i,z} \in \{\pm 1\}$ coupled to XY phase-variables $\theta_{z,i} = \text{Arg} \Delta_z(\vec{r}_i) \in [0, 2\pi]$ where z labels physical layers, i labels lattice sites in the xy-plane, and $J(\sigma_{z,i}, \sigma_{z,j}) \equiv J_0 (1 + \sigma_{z,i})(1 + \sigma_{z,j})/4$.

In the lattice model, $\sigma_z = +1$ ($\sigma_z = -1$) indicates that layers z and $z+1$ are paired (un-paired respectively). The uniformly dimerized ground state of the multilayer system corresponds to anti-ferromagnetic Ising order along the z-axis and ferromagnetic order within the xy-plane. Ising domain walls correspond to regions where pairing switches between the two equivalent dimerization configurations over a distance of the order of the GL coherence length, either along the z-axis or within the xy-plane. The coupling constants K_z and K_\perp reflect the energy cost of deforming the magnitude of the pairing order parameter, $|\Delta|$, to form a domain wall along the z-axis or in the xy-plane respectively (see Fig. 2).

The coupling $J(\sigma_{z,i}, \sigma_{z,j})$ corresponds to the average superfluid stiffness $\rho \sim \kappa |\Delta|^2$ in the vicinity of lattice site (i, z) and determines the energy cost of twisting the phase of the order parameter, $\theta_{z,i}$, between sites i and j in the same plane. The local stiffness is non-zero wherever $\sigma_{z,i} = +1$, and zero otherwise [12].

The lattice model couplings (K_z, K_\perp, J_0) can be estimated from the GL model. An in-plane dimerization domain wall along the x-direction (Fig. 2b) corresponds to pairing configurations of the form $\Delta_z(x) = \frac{\Delta_0}{2} [1 + (-1)^z \alpha(x)]$ where $\Delta_0^2 = \frac{|r|}{2u}$, and $\alpha(x)$ is a function that changes from -1 to $+1$ around $x = 0$, and tends

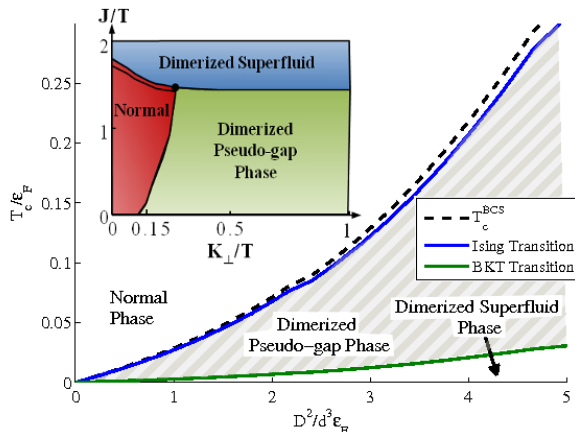


FIG. 3. The lattice model phase-diagram, calculated using the temperature dependence of the GL coefficients in (3) and plotted in terms of dipole interaction strength D^2/d^3 and temperature T , each measured in units of ϵ_F (main figure). Phase diagram predicted by the effective lattice model for generic model parameters, with $K_z/K_\perp = 2$. Double line indicates first-order transition (inset).

to a constant away from $x = 0$. Minimization of the free energy with respect to $\alpha(x)$ yields $\alpha(x) = \tanh(2x/\ell_{DW})$ where $\ell_{DW} \equiv \sqrt{\frac{32\kappa}{3r}}$ [12]. The corresponding free energy cost per unit length is $U_{DW}^{(\perp)} = \ell_{DW} \frac{|r|^2}{8u}$.

There are two possible z -axis domain wall configurations, shown in Fig. 2c,d. To determine their free energy cost, we consider a system with periodic boundary conditions along the z axis, and compare the free energy of the ground state to that of the domain wall configurations. This yields an energy cost per unit area $U_{DW}^{(z)} = \frac{|r|^2}{8u}$ for both types of domain walls. Setting the lattice spacing equal to ℓ_{DW} , the energetics of in-plane and z -axis domain walls are reproduced by $K_z = 2K_\perp = \frac{4\kappa|r|}{3u}$. In order to determine the lattice phase stiffness J_0 , we equate the cost of an infinitesimal phase twist, $\theta_{z,j} = \theta_{z,i} + \delta\theta$, in a fully paired layer ($\sigma_z = 1$) to the corresponding cost in the GL free energy (Eq. 2). This gives $J_0 = \frac{\kappa|r|}{u}$.

The lattice model (Eq. 3) describes three-dimensional Ising spins coupled to many independent two-dimensional XY layers. For temperatures near or below the Ising transition temperature, the Ising variables have large correlation lengths and hence see an average over many independent layers of XY spins. With this self-averaging property in mind, we decouple the XY and Ising variables in a mean-field factorization

$$F_\sigma = K_z \sum_{(zz'),i} \sigma_{zi} \sigma_{z'i} - K_\perp^{(\text{eff})} \sum_{z,(ij)} \sigma_{zi} \sigma_{zj} - h \sum_{z,i} \sigma_{zi}$$

$$F_{XY} = - \sum_{(ij)} \frac{J_0}{4} [1 + (-1)^z \sigma_0]^2 \cos(\theta_{z,i} - \theta_{z,j})$$

where $K_\perp^{(\text{eff})} = K_\perp + \frac{J_0}{4} \left(\frac{A+B}{2} \right)$ and $A, B \equiv \langle \cos(\theta_i^{(e/o)} - \theta_j^{(e/o)}) \rangle_{F_{XY}} - 1$ are the averages (with respect to F_{XY})

of the cosine terms in even and odd layers respectively, $\sigma_0 \equiv \langle \sigma \rangle_{F_\sigma}$, and $h = \left(\frac{A-B}{2} \right) \frac{J_0}{2}$.

The decoupled Ising model and XY models can then be analyzed separately but self-consistently. A mean-field analysis is adequate for 3D Ising model. The phase action is treated by a variational self-consistent harmonic approximation (SCHA) [13]. While the SCHA provides a reasonable estimate of the location of the 2D BKT transition, it spuriously predicts a strong first-order transition in which $\langle F_{XY} \rangle_{\text{SCHA}}$ drops abruptly to zero at the XY transition temperature, T_{XY} . At higher temperatures, the SCHA dramatically underestimates the contribution to energy density from phase fluctuations. In order to avoid this undesirable feature, we supplement the SCHA value for $\langle \cos \Delta_{ij} \theta \rangle_{\text{SCHA}}$ with a high-temperature expansion for $T > T_{XY}$:

$$\langle \cos \Delta_{ij} \theta^{(z)} \rangle = \begin{cases} \langle \cos \Delta_{ij} \theta^{(z)} \rangle_{\text{SCHA}} & ; T < T_{XY} \\ J(\sigma_0, \sigma_0)/2T & ; T > T_{XY} \end{cases} \quad (4)$$

Fig. 3 shows the phase diagram predicted by the effective lattice model. The main figure displays the phase diagram where the model parameters are taken from the GL coefficients in (3). The BCS transition temperature, T_c^{BCS} , is obtained by solving numerically the BCS gap equation for the dipole potential. Whereas the dimerization transition occurs close to the mean-field BCS transition temperature, T_c^{BCS} , the BKT transition to phase QLRO occurs at a lower temperature, leaving an intermediate region with full dimerization but only short range superfluid correlations.

Recent experiments on 3D clouds of ultra-cold $^{40}\text{K}^{87}\text{Rb}$ molecules have achieved densities on the order of $n_{3d} = 10^{12} \text{cm}^{-3}$ and permanent electrical dipole moments of up to 0.566 Debye [6]. If similar densities were achieved in a layered system with layer spacing on the order of 400nm, the ratio of typical dipole interactions to Fermi-energy would be $D^2/(4\pi\epsilon_0 d^3 \epsilon_F) \sim 3$.

While the GL parameters in Eq. 2 provide an initial estimate of the lattice-model coupling constants, in principle, the model coefficients can be renormalized by higher order terms in the GL expansion. The inset shows the phase diagram for generic values of the model parameters K_\perp and J_0 with $K_z/K_\perp = 2$ (the qualitative features do not depend sensitively this ratio). An additional feature emerges for generic coefficients: for J sufficiently bigger than K , there is a tri-critical point where the BKT and Ising transitions fuse into a weakly first-order phase transition.

Order parameter and detection - The dimerized phase breaks translational symmetry in the z direction. It can be characterized by the following *four fermion* order parameter: $\mathcal{D} = \langle n_{z-1,r} n_{z,r} - n_{z,r} n_{z+1,r} \rangle$, where $n_{z,r} = \psi_{z,r}^\dagger \psi_{z,r}$ is the local fermion density. For finite transverse confinement, in the dimerized phase, every two paired layers shift slightly towards each other. The

displacement scales as $\delta z \propto \Omega_z^{-2}$, where Ω_z is the layer-confinement frequency in the z -direction. The dimerized phase can be detected by the appearance of new Bragg peaks in elastic light scattering (see Fig. 1) with wavevector $\mathbf{Q} = n\pi\hat{\mathbf{z}}/d$, $n = 1, 3, \dots$, with intensity $\sim \delta z^2$.

In the strong-confinement limit, $\Omega_z \rightarrow \infty$, the particle density does not show any sign of dimerization. However in this regime, the dimerized phase could still be detected by measuring correlations between the amplitudes of light scattered at different wavevectors: $\langle n_{\mathbf{q}} n_{\mathbf{q}'} \rangle \propto n_0^2 \delta_{\mathbf{q}+\mathbf{q}'} + \delta_{\mathbf{Q}-\mathbf{q}-\mathbf{q}'} \mathcal{D}$, where \mathbf{q} and \mathbf{q}' are two scattering wavevectors and n_0 is a constant.

Three Layer Case - The three layer system is a special case that requires more careful analysis. If one proceeds as above and includes interactions only between neighboring layers, the system possesses an extra $SU(2)$ symmetry generated by: $I^z = \int d^2r (\psi_3^\dagger \psi_3 - \psi_1^\dagger \psi_1)$ and $I^\pm = \int d^2r (\psi_3^\dagger \psi_1 \pm i \psi_1^\dagger \psi_3)$. The $U(1)$ generator $N_2 = \int d^2r \psi_2^\dagger \psi_2$ completes the $SU(2)$ symmetry to $U(2)$. These generators commute with $\mathcal{H} = \mathcal{H}_{\text{kin}} + V_{12} + V_{23}$, where V_{ij} is the interaction between layers i and j . This $U(2)$ symmetry dictates that, to all orders in the GL expansion, the free energy should be a function of $(|\Delta_1|^2 + |\Delta_2|^2)$ only, which does not energetically distinguish dimerization from uniform pairing.

However intralayer and next-nearest neighbor interactions $\tilde{V} = V_{13} + \sum_{j=1}^3 V_{jj}$ break the $SU(2)$ symmetry of the three layer system, and generate a quartic term of the form $-|v||\Delta_1|^2|\Delta_2|^2$ in the GL free energy. This term is relevant [14] (in the renormalization group sense) and hence, we expect the trilayer system to exhibit uniform pairing with $|\Delta_1| = |\Delta_2|$. In contrast, for $N_{\text{Layers}} > 3$, already the dominant nearest neighbor interactions strongly favor dimerization and \tilde{V} only produce small subleading corrections.

Discussion - Our analysis of the layered dipolar Fermi system predicts a sequence of two phase-transitions: an Ising-like dimerization transition followed by a BKT transition to phase QLRO. One can generalize to one-dimension, and consider a stack of one-dimensional tubes of dipolar fermions [15]. In this case, no phase ordering can occur at any finite temperature, since the phase dynamics are strictly one-dimensional. However, a dimerization transition is still possible, leading to wider range of dimerized, non-superfluid phase [16].

We expect that the Ising-XY model description of the layered dipolar fermions will be insufficient deep in the BEC regime where interaction energies are dominant compared to the Fermi-energy. For sufficiently strong interactions or sufficiently dense systems, the system will form a Wigner crystal [17]. Another possibility is that the formation of longer chains of three or more dipoles may become important [9]. In a regime where chains of n dipoles are favorable, a many-layered system would

undergo n -merization rather than dimerization. Correspondingly, an n -merized phase may undergo an n -state clock-model-type phase transition which generalizes the Ising-type dimerization transition considered above. Furthermore, for even n , bosonic chains could condense into an exotic superfluid of dipolar chains. Such states offer an intriguing chance to examine the relatively unexplored boundary between few-body interactions and many-body phase transitions, and deserve further study.

Acknowledgements - We would like to acknowledge: E. Altman, T. Giamarchi, M. Lukin, D.F. Mross, D. Podolsky and S. Sachdev for helpful conversations. This work was supported by: NSF IGERT Grant No. DGE-0801525, NSF grants DMR-0705472 and DMR-0757145, AFOSR Quantum Simulation MURI, AFOSR MURI on Ultracold Molecules, DARPA OLE program, Harvard-MIT CUA, NSF grant DMR-09-06475.

-
- [1] M Baranov et al 2002 Phys. Scr. 2002 74; J. Doyle et al., Eur. Phys. J.D 31, 149 (2004); T Lahaye et al., Rep. Prog. Phys. 72, 126401 (2009); M. Baranov, Physics Reports 464, 71 (2008); M. A. Baranov, M. S. Marenko, V. S. Rychkov, and G. V. Shlyapnikov, Phys. Rev. A 66, 013606 (2002)
 - [2] N. R. Cooper and G. V. Shlyapnikov, Phys. Rev. Lett. 103, 155302 (2009).
 - [3] J. Quintanilla, S.T. Carr, and J.J. Betouras, Phys. Rev. A 79, 031601(R) (2009); B. M. Fregoso, K. Sun, E. Fradkin, and B. Lev, New J. Phys. 11, 103003 (2009); S.T. Carr, J. Quintanilla, and J.J. Betouras, Phys. Rev. B 82, 045110 (2010); .
 - [4] A. Micheli, G. K. Brennen and P. Zoller, Nature Physics 2, 341 - 347 (2006).
 - [5] P. Rabl et al., Phys. Rev. Lett. 97, 033003 (2006)
 - [6] K.K. Ni et al., Science 322, 231 (2008); J. Stuhler et al., Phys. Rev. Lett. 95, 150406 (2005); K. Pilch et al., Phys. Rev. A 79, 042718 (2009).; S. Ospelkaus et al., Faraday Discuss. 142, 351 (2009).
 - [7] L. Santos, G. V. Shlyapnikov, P. Zoller, and M. Lewenstein Phys. Rev. Lett. 85, 1791 (2000)
 - [8] D.W. Wang, Phys. Rev. Lett. 98, 060403 (2007).
 - [9] D.W. Wang, M.D. Lukin, and E. Demler Phys. Rev. Lett. 97, 180413 (2006); M. Klawunn, J. Duhme, L. Santos, arXiv:0907.4612v1 (2009).
 - [10] See, for example, A.V. Chubukov, Phys. Rev. B. 44, 4693(R) (1991); N. Shannon, T. Momoi, and P. Sindzingre, Phys. Rev. Lett. 96, 027213 (2006).
 - [11] C. Wu, Phys. Rev. Lett. 95, 266404 (2005); E. Berg et al., Nature Phys. 5, 830 (2009).
 - [12] See supplementary materials for further details.
 - [13] Giamarchi, T., 2004, Quantum Physics in One Dimension (Oxford University Press, Oxford).
 - [14] R. A. Pelcovits and D. R. Nelson Phys. Lett. 57A, 23 (1976).
 - [15] C. Kollath, J. S. Meyer, and T. Giamarchi, Phys. Rev. Lett. 100, 130403 (2008)
 - [16] In 1D, where the Fermi-surface is perfectly nested, one must also consider possible charge ordered states.
 - [17] H. P. Büchler et al., Phys. Rev. Lett. 98, 060404 (2007);

M. A. Baranov, H. Fehrmann, and M. Lewenstein, Phys. Rev. Lett. 100, 200402 (2008).

- [18] E. Granato, J. M. Kosterlitz, J. Lee, and M. P. Nightingale, Phys. Rev. Lett. **66**, 1090 (1991); P. Olsson Phys. Rev. Lett. **75**, 2758 (1995).

Appendix A. BCS Gap Equation for Bilayer

In this section, we show that the attractive component of intralayer dipolar interaction induces BCS pairing in a bilayer system. We ignore repulsive intralayer interactions, as these serve only to renormalize the Fermi liquid parameters of the dipolar system. The interaction between dipoles in adjacent layers separated by interlayer spacing d along the z -axis, and by distance r in the xy -plane, and with dipole moments D polarized along the z -axis by an external field is:

$$V_{\text{dip}}(r) = \frac{D^2}{(r^2 + d^2)^{3/2}} \left(1 - \frac{3d^2}{r^2 + d^2} \right) \quad (5)$$

where we work in units with $4\pi\epsilon_0 = 1$. Fourier transforming (5) with respect to in-plane coordinate r , one finds:

$$V_q^{(z,z+1)} = -D^2 q e^{-qd} \quad (6)$$

We assume that pairing in the s-wave channel dominates, and that the transition temperature is set by condensation of Cooper pairs with zero center of mass momentum. The self-consistency equation for the BCS order parameter Δ at temperature T reads:

$$\begin{aligned} \Delta_{z,\mathbf{k}} &= - \sum_{\mathbf{k}'} V_{|\mathbf{k}-\mathbf{k}'|}^{(z,z+1)} \langle \psi_{z+1,-\mathbf{k}'} \psi_{z,\mathbf{k}'} \rangle \\ &= - \frac{1}{2} \sum_{\mathbf{k}'} \frac{V_{|\mathbf{k}-\mathbf{k}'|}^{(z,z+1)} \Delta_{z,\mathbf{k}'}}{E_{\mathbf{k}'}} \tanh \left(\frac{E_{\mathbf{k}'}}{2T} \right) \end{aligned} \quad (7)$$

In (7), $E_{\mathbf{k}} = \sqrt{\xi_{\mathbf{k}}^2 + \Delta_{z,\mathbf{k}}^2}$ where $\xi_{\mathbf{k}} = \frac{k^2}{2m} - \mu$, m is the effective mass, and μ is the chemical potential. Since the number of particles on each layer is fixed, one must simultaneously solve for Δ using (7) and for μ by fixing the particle density n :

$$n = \sum_{\mathbf{k}} \left[1 - \frac{\xi_{\mathbf{k}}}{E_{\mathbf{k}}} \tanh \left(\frac{E_{\mathbf{k}}}{2T} \right) \right] \quad (8)$$

We solve (7,8) numerically, using the expression (6) for the dipole potential, and find a non-zero solution for any dipole moment D . Fig. (4)a. shows the $T = 0$ solution for Δ as a function of interaction strength $D^2/d^3\epsilon_F$, and Fig. (4)b. shows the temperature profile of the BCS gap for various interactions strengths. These results demonstrate that intralayer interactions induce pairing for any value of dipole interaction strength.

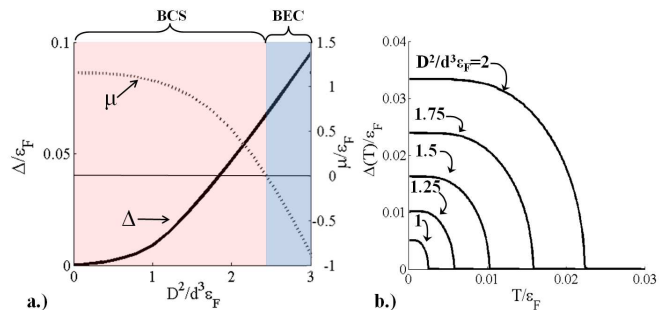


FIG. 4. (color online) Numerical solutions of the BCS gap equation (7) for the nearest-neighboring layer dipole potential (6), at fixed particle density, and with $d/\lambda_F = 1$, where $\lambda_F = 2\pi/k_F$ is the Fermi wavelength. (a) $T = 0$ BCS pairing as a function of interaction strength D^2/d^3 (where energies are measured with respect to the Fermi energy ϵ_F of the unpaired system). Solid line shows solution for Δ , and dotted line shows chemical potential μ . The BCS regime ($\mu > 0$) and BEC regime ($\mu < 0$) are highlighted in red and blue respectively. (b) Temperature profile of the BCS gap for interaction strengths: $D^2/d^3\epsilon_F = 2, 1.75, 1.5, 1.25,$ and 1 (highest to lowest respectively).

In addition, one of us (D.W. Wang) has performed detailed studies of BCS pairing in $\mathcal{N} = 2, 3,$ and 4 layer systems. These studies confirm that interlayer pairing occurs in these few-layered structures, and demonstrate explicitly that dimerization is favored for $\mathcal{N} = 4$, but not for $\mathcal{N} = 3$, in agreement with our analytic results from the Ginzburg-Landau free energy. This work will be published elsewhere.

Appendix B. Derivation of Ginzburg-Landau Free-Energy

In this section, we include for completeness, details of the derivation of the Ginzburg-Landau (GL) free-energy (2) from the microscopic fermionic action (1) for an \mathcal{N} layer system. This derivation, based on the Hubbard-Stratanovich (H-S) transformation, follows a standard route to deriving the GL free-energy in BCS theory (see for example A. Altland and B. Simons, Condensed Matter Field Theory (Cambridge University Press, Cambridge, 2006) p. 271-309).

Starting with (2) we introduce H-S fields $\Delta_z(\mathbf{k}_\perp, \mathbf{Q}_\perp) = - \sum_{\mathbf{k}'} V_{|\mathbf{k}-\mathbf{k}'|}^{(z,z+1)} \langle \psi_{z+1,-\mathbf{k}'+\mathbf{Q}/2} \psi_{z,\mathbf{k}'+\mathbf{Q}/2} \rangle$. The subscript z labels layer, and the two momentum labels $(\mathbf{k}_\perp, \mathbf{Q}_\perp)$ refer to the relative displacement and center of mass motion of the Cooper pairs respectively. The inclusion of $\mathbf{Q}_\perp \neq 0$ allows for spatial variations of the order parameters Δ_z .

With the introduction of the H-S fields Δ_z , the

fermionic action now reads:

$$S = \sum_{z,k,k',Q} \Delta_{z,k,Q} (V^{-1})_{k,k'} \Delta_{z,k',Q} + \sum_{k,Q} \Psi_{k,Q}^\dagger \mathcal{H}_\Delta \Psi_{k,Q} \quad (9)$$

$$\mathcal{H}_\Delta = \begin{pmatrix} i\omega + \xi & \Delta_{1,k,Q} & 0 & \cdots \\ \bar{\Delta}_{1,k,Q} & i\omega - \xi & -\bar{\Delta}_{2,-k,Q} & \cdots \\ 0 & -\Delta_{2,k,Q} & i\omega + \xi & \cdots \\ \vdots & \vdots & \vdots & \ddots \end{pmatrix} \quad (10)$$

where $\Psi_{k,Q} \equiv (\bar{\psi}_{1,-k+Q} \ \psi_{2,k} \ \bar{\psi}_{3,-k+Q} \ \psi_{4,k} \ \dots)^T$, and ω is an (imaginary) Matsubara frequency label. Here, $(V^{-1})_{k,k'}$ denotes (k, k') component of the inverse (in the operator sense) of the dipole potential (6). As will be explained below, it is not necessary to explicitly compute this inverse in order to develop the GL theory. Since we

are concerned with finite temperature phase transitions, we neglect quantum fluctuations by treating Δ as independent of ω . This corresponds to developing the GL free-energy for the $\omega = 0$ component of Δ_z . We also assume that the relative displacement momentum k profile of $\Delta_{k,Q}$ does not fluctuate substantially from the mean-field form. This corresponds to fixing the form of the Cooper pair wave-function to the one most energetically favored at the mean-field level, and is justified by the fact that the dominant instability towards pairing will occur with this pairing profile. With this assumption, the k labels on Δ are non-dynamical and will be dropped from subsequent expressions. We have validated this approach by checking that the resulting GL free-energy derived in this way can accurately reproduce the results of the numerical solution to the BCS gap-equation.

Integrating out the Fermions gives the following effective action for the Hubbard-Stratonovich fields Δ_z :

$$\begin{aligned} S[\Delta] &= \sum_n S^{(2n)}[\Delta] = \text{Tr} \ln [1 + G_0^{-1} \mathcal{H}_\Delta] = \\ &= \sum_{n=1}^{\infty} \frac{1}{2n} \text{Tr} \left[\begin{pmatrix} G_0^h & 0 & 0 & \cdots \\ 0 & G_0^p & 0 & \cdots \\ 0 & 0 & G_0^h & \cdots \\ \vdots & \vdots & \vdots & \ddots \end{pmatrix} \begin{pmatrix} 0 & \Delta_1(Q) & 0 & \cdots \\ \bar{\Delta}_1(Q) & 0 & -\bar{\Delta}_2(Q) & \cdots \\ 0 & -\Delta_2(Q) & 0 & \cdots \\ \vdots & \vdots & \vdots & \ddots \end{pmatrix} \right]^{2n} \\ &= \sum_{n=1}^{\infty} \frac{1}{2n} \text{Tr} \left[\begin{pmatrix} 0 & \Delta_1 & 0 & 0 & \cdots & 0 & 0 \\ \bar{\Delta}_1 & 0 & -\bar{\Delta}_2 & 0 & \cdots & 0 & 0 \\ 0 & -\Delta_2 & 0 & \Delta_3 & \cdots & 0 & 0 \\ \vdots & \vdots & \vdots & \vdots & \ddots & \vdots & \vdots \\ 0 & 0 & 0 & 0 & \cdots & 0 & \Delta_{\mathcal{N}} \\ 0 & 0 & 0 & 0 & \cdots & \bar{\Delta}_{\mathcal{N}} & 0 \end{pmatrix}^2 G_{0,k}^p G_{0,-k+Q}^h \right]^n \\ &= \sum_{n=1}^{\infty} \frac{1}{2n} \text{Tr} \left[\begin{pmatrix} |\Delta_1|^2 & 0 & -\Delta_1 \bar{\Delta}_2 & 0 & \cdots & 0 & 0 \\ 0 & |\Delta_1|^2 + |\Delta_2|^2 & 0 & -\bar{\Delta}_2 \Delta_3 & \cdots & 0 & 0 \\ -\Delta_2 \bar{\Delta}_1 & 0 & |\Delta_2|^2 + |\Delta_3|^2 & 0 & \cdots & 0 & 0 \\ \vdots & \vdots & \vdots & \vdots & \ddots & \vdots & \vdots \\ 0 & 0 & 0 & 0 & \cdots & |\Delta_{\mathcal{N}-2}|^2 + |\Delta_{\mathcal{N}-1}|^2 & 0 \\ 0 & 0 & 0 & 0 & \cdots & 0 & |\Delta_{\mathcal{N}}|^2 \end{pmatrix} G_{0k}^p G_{0,-k+Q}^h \right]^n \end{aligned} \quad (11)$$

where we have dropped all irrelevant constant terms that do not depend on Δ , and $G_{0,k}^p = \frac{1}{i\omega - \xi_k}$, $G_{0,k}^h = \frac{1}{i\omega + \xi_k}$ are the particle and hole Green functions respectively (note the precise form of the bottom right entry of the second line of (11) depends on whether \mathcal{N} is odd or even). Also, in (11) momentum labels on Δ and G_0 have been suppressed where possible in order to conserve space.

We truncate the above series at quartic order, which is formally justified near the pairing transition tem-

perature T_c^{MF} where Δ is small. The GL coefficients $\{\kappa, r, u\}$ can then be computed by explicitly evaluating the trace over the products of fermion Green functions appearing in (11). The terms quadratic in Δ are: $S^{(2)} = \sum_q \Gamma_Q^{-1} |\Delta(Q)|^2$ where $\Gamma(Q, T) \equiv V^{-1} - \frac{T}{\Omega} \sum_p G_{0,p}^p G_{0,-p+Q}^h$, and where Ω is the system volume. The mass term, with coefficient r , determines the energy of having a uniform pairing amplitude $|\Delta|$. To compute r , we note that at T_c^{MF} we have: $\Gamma(0, T_c^{\text{MF}}) = 0 =$

$V^{-1} - \frac{T_c^{\text{MF}}}{\Omega} \sum_p G_{0,p}^p G_{0,-p}^h$, indicating that for T near T_c^{MF} one can expand:

$$\begin{aligned} r &= (T - T_c^{\text{MF}}) \frac{-\partial}{\partial T} \sum_p G_{0,p}^p G_{0,-p}^h \\ &= (T - T_c^{\text{MF}}) \int \frac{d^2 p}{(2\pi)^2} \frac{-\partial_T n_F(\xi_p, T_c^{\text{MF}})}{\xi_p} \\ &= \nu t \end{aligned} \quad (12)$$

where $n_F(\varepsilon, T)$ is the Fermi-distribution at energy $\varepsilon - \mu$ and temperature T . The coefficient κ , of the gradient term $\kappa |\nabla_{\perp} \Delta|^2$, is obtained by expanding $\Gamma(Q, T)$ to quadratic order in Q :

$$\begin{aligned} \kappa &= \frac{\partial}{\partial Q^2} \left[-\frac{T}{\Omega} \sum_p G_{0,p} G_{0,-p+Q} \right] \\ &= \frac{\partial}{\partial Q^2} \int \frac{d^2 p}{(2\pi)^2} \left(\frac{\mathbf{Q} \cdot \mathbf{p}}{2m} \right)^2 \frac{-\partial_{\xi}^2 n_F(\xi_p, T)}{2\xi_p} = \frac{7\zeta(3)}{32\pi^3} \frac{\varepsilon_F}{T^2} \end{aligned} \quad (13)$$

Note that obtaining κ and r by expanding $\Gamma(Q, T)$ to leading order in Q and T respectively has allowed us to neatly sidestep the explicit computation of V^{-1} . Another interesting feature is that the details of the dipole potential are fully contained in the single parameter, T_c^{MF} , which we obtain by numerically solving (7).

Finally, we turn to the evaluation of the quartic term coefficient u , which comes from terms of the form $S^{(4)} \sim |\Delta|^4 \sum_p (G_p^p G_{-p}^h)^2$. The Matsubara frequency summation in $\sum_p (G_p^p G_{-p}^h)^2$ can be done explicitly:

$$\begin{aligned} &\sum_{\omega_n} \frac{1}{(i\omega_n - \xi_p)^2} \frac{1}{(i\omega_n + \xi_p)^2} \\ &= \oint \frac{-dz}{2\pi i} \frac{\beta}{e^{\beta z} + 1} \frac{1}{(z - \xi_p)^2} \frac{1}{(z + \xi_p)^2} \\ &= \frac{-\beta^2}{8\xi_p^2 \cosh^2(\beta\xi_p/2)} + \frac{\beta}{4\xi_p^3} \tanh(\beta\xi_p/2) \end{aligned} \quad (14)$$

where $\beta = 1/T$ is the inverse temperature. The remaining integral over \vec{p} can be rendered dimensionless and computed numerically yielding:

$$\kappa = \frac{\nu\beta^3}{32} \int_{-\infty}^{\infty} dx \left(-\frac{1}{x^2 \cosh^2 x} + \frac{\tanh x}{x^3} \right) = \frac{1.7}{32} \frac{\nu}{T^3} \quad (15)$$

Using the above computations of $\{\kappa, r, u\}$ it is now a straightforward matter to evaluate (11), which for infinite number of layers gives:

$$\begin{aligned} F &= \sum_z \int d^2 r \left(\kappa |\nabla_{\perp} \Delta_z|^2 + r |\Delta_z|^2 \right. \\ &\quad \left. + u |\Delta_z|^4 + 2u |\Delta_z|^2 |\Delta_{z+1}|^2 \right) \end{aligned} \quad (16)$$

The relative factor of 2 between the $|\Delta_z|^4$ and $|\Delta_z|^2 |\Delta_{z+1}|^2$ terms can be obtained by a careful accounting of combinatorics. Alternatively, this factor may be checked by considering a trilayer system whose microscopic $SU(2)$ symmetry (described in the main text) guarantees that the quartic terms in the GL free energy be of the form: $S_{\mathcal{N}=3}^{(4)} = u(|\Delta_1|^2 + |\Delta_2|^2)^2$.

Appendix C. Coupling Between Domain Walls and Phase Fluctuations

In this section, we discuss some subtleties involved in coarse graining the GL free-energy (2) to arrive at the effective lattice model (3). In deriving the value of the XY stiffness $J(\sigma_i, \sigma_j)$, which couples the dimerization order parameter to phase fluctuations, we have made the simplifying approximation that the the superfluid stiffness drops abruptly to zero at the location of an in-plane Ising domain wall.

In reality, there is some residual superfluid stiffness that varies continuously across the length of the domain wall. Keeping track of this residual stiffness corresponds to including higher order gradient terms such as $\kappa^{(2)} |\nabla_{\perp} \Delta_z(r)|^4$, which includes terms of the form $|\Delta|^2 |\nabla_{\perp} \Delta(r)|^2 |\nabla \theta(r)|^2$ that couple domain walls and phase fluctuations. However, these terms are subleading and have a negligible effect on the systems phase diagrams. Formally, this is because such higher order gradient terms are highly irrelevant in the renormalization group sense.

We have also conducted separate simulations that include residual phase stiffness at the dimerization domain boundaries, and have explicitly confirmed that the resulting phase diagram is highly insensitive to the inclusion of such terms. Specifically, in addition to the usual $J(\sigma_i = +1, \sigma_j = +1) = J_0$ and $J(-1, -1) = 0$, we allowed for $J(+1, -1) = J(-1, +1) = J_{\text{res}}$, and verified that the choice of value for J_{res} had little discernible effect on either the dimerization or BKT phase transitions.

A second simplifying assumption is used in parameterizing the in-plane domain wall as $\Delta(x) = \frac{|\Delta_0|}{2}(1 + \alpha(x))$. This parameterization implicitly assumes constant phase over the range of the domain wall, which is justified because $\ell_{\text{DW}} \sim \xi_{\text{GL}}$. Since ξ_{GL} is the shortest scale over which the phase is well-defined, it is essentially constant on lengthscales $\leq \xi_{\text{GL}}$.